Available online at www.sciencedirect.com
SCIENCE DIRECT®
Toxicology in Vitro 19 (2005) 975–983
Toxicology in Vitro
www.elsevier.com/locate/toxinvit

In vitro toxicity of nanoparticles in BRL 3A rat liver cells

S.M. Hussain [a,*], K.L. Hess [b], J.M. Gearhart [c], K.T. Geiss [d], J.J. Schlager [a]

[a] Applied Biotechnology, Air Force Research Laboratory/HEPB, Wright-Patterson AFB, OH, USA
[b] Geo-Centers, Inc., Wright-Patterson AFB, OH, USA
[c] Alion Science & Technology, Wright-Patterson AFB, P.O. Box 31009, Dayton, OH 45431-0009, USA
[d] Human Effectiveness Directorate, Air Force Research Laboratory, Wright-Patterson AFB, OH, USA

Received 31 March 2005; accepted 17 June 2005
Available online 25 August 2005

Abstract

This study was undertaken to address the current deficient knowledge of cellular response to nanosized particle exposure. The study evaluated the acute toxic effects of metal/metal oxide nanoparticles proposed for future use in industrial production methods using the in vitro rat liver derived cell line (BRL 3A). Different sizes of nanoparticles such as silver (Ag; 15, 100 nm), molybdenum (MoO_3; 30, 150 nm), aluminum (Al; 30, 103 nm), iron oxide (Fe_3O_4; 30, 47 nm), and titanium dioxide (TiO_2; 40 nm) were evaluated for their potential toxicity. We also assessed the toxicity of relatively larger particles of cadmium oxide (CdO; 1 μm), manganese oxide (MnO_2; 1–2 μm), and tungsten (W; 27 μm), to compare the cellular toxic responses with respect to the different sizes of nanoparticles with different core chemical compositions. For toxicity evaluations, cellular morphology, mitochondrial function (MTT assay), membrane leakage of lactate dehydrogenase (LDH assay), reduced glutathione (GSH) levels, reactive oxygen species (ROS), and mitochondrial membrane potential (MMP) were assessed under control and exposed conditions (24 h of exposure). Results showed that mitochondrial function decreased significantly in cells exposed to Ag nanoparticles at 5–50 μg/ml. However, Fe_3O_4, Al, MoO_3 and TiO_2 had no measurable effect at lower doses (10–50 μg/ml), while there was a significant effect at higher levels (100–250 μg/ml). LDH leakage significantly increased in cells exposed to Ag nanoparticles (10–50 μg/ml), while the other nanoparticles tested displayed LDH leakage only at higher doses (100–250 μg/ml). In summary the Ag was highly toxic whereas, MoO_3 moderately toxic and Fe_3O_4, Al, MnO_2 and W displayed less or no toxicity at the doses tested. The microscopic studies demonstrated that nanoparticle-exposed cells at higher doses became abnormal in size, displaying cellular shrinkage, and an acquisition of an irregular shape. Due to toxicity of silver, further study conducted with reference to its oxidative stress. The results exhibited significant depletion of GSH level, reduced mitochondrial membrane potential and increase in ROS levels, which suggested that cytotoxicity of Ag (15, 100 nm) in liver cells is likely to be mediated through oxidative stress.

Keywords: Nanoparticles; In vitro toxicity; Oxidative stress

1. Introduction

Nanotechnology involves the creation and manipulation of materials at nanoscale levels to create products that exhibit novel properties. Recently, nanomaterials such as nanotubes, nanowires, fullerene derivatives (buckyballs) and quantum dots have received enormous attention to create new types of analytical tools for biotechnology and life sciences (Bruchez et al., 1998; Taton et al., 2000; Cui et al., 2001). Nanomaterials, which range in size from 1 to 100 nm, have been used to create unique devices at the nanoscale level possessing novel physical and chemical functional properties (Colvin, 2003; Oberdörster, 2004). Although nanomaterials are currently being widely used in modern technology, there

* Corresponding author. Address: Applied Biotechnology, Air Force Research Laboratory/HEPB, Area B, R ST, BDL 837, Wright-Patterson Air Force Base, AFB, Dayton, OH-45433-5707, USA. Tel.: +1 937 904 9517; fax: +1 937 904 9610.
E-mail address: saber.hussain@wpafb.af.mil (S.M. Hussain).

0887-2333/$ - see front matter © 2005 Elsevier Ltd. All rights reserved.
doi:10.1016/j.tiv.2005.06.034

is a serious lack of information concerning the human health and environmental implications of manufactured nanomaterials. The major toxicological concern is the fact that some of the manufactured nanomaterials are redox active (Colvin, 2003), and some particles transport across cell membranes and especially into mitochondria (Foley et al., 2002). One of the few relevant studies was with single-wall carbon nanotubes in mice (Lam et al., 2004). Lam et al. (2004) demonstrated that carbon nanotube products induced dose-dependent epithelioid granulomas in mice and, in some cases, interstitial inflammation in the animals of the 7-day post-exposure groups. The recent study by Oberdörster (2004) indicated that nanomaterials (Fullerences C_{60}) induced oxidative stress in a fish model. Although limited studies have been conducted on the toxicity of nanoparticles, there are no reports on the use of in vitro models to evaluate potential toxicity screening of nanomaterials. The BRL 3A immortal rat liver cell line was selected in the present study as a convenient in vitro model to assess nanocellular toxicity. This cell line has been well characterized for its relevance to toxicity models (Boess et al., 2003). In vivo exposure to nanoparticles is likely to have potential impact on the liver since exposure to these particles is likely to occur through ingestion and clearance by the liver (Jani et al., 1990). The toxicity end points (MTT, LDH, ROS and GSH) that were selected in the current study represent vital biological functions of the mammalian system as well as provide a general sense of toxicity in a relatively short time. The results described in this paper provide a range of doses that were toxic to these cultured cells and data pointing to a general mechanism of nanoparticle toxicity. Since little information is available on nanomaterial toxicity, simple in vitro toxicity models and general toxicity end points are likely to assist in mechanistic events after exposure and subsequent toxicity risk assessment of nanomaterials.

2. Materials and methods

2.1. Chemicals

The test materials silver (Ag; 15, 100 nm), molybdenum (MoO_3; 30, 150 nm), aluminum (Al; 30, 103 nm), iron oxide (Fe_3O_4; 30, 47 nm), manganese oxide (MnO_2; 1–2 μm), and tungsten (W; 27 μm) were received from Air Force Research Laboratory, Brooks AFB, TX. Cadmium oxide (CdO-1000 nm) and titanium oxide (TiO_2-40 nm) were purchased from Fluka Chemicals and Altair, Nanomaterials Inc., respectively. The 3-(4,5-Dimethylthiazol-2-yl)-2,5-diphenyltetrazolium bromide (MTT), β-nicotinamide-adenine dinucleotide-reduced (NADH), reduced GSH, rhodamine 123, Ham's nutrient mixture F-12 media and gentamycin, were purchased from Sigma Chemical Company (St. Louis, MO).

2.2. Dispersion of nanomaterials in solution

The dispersion test was conducted in physiological phosphate buffer saline (PBS) or deionized water. Based on success of homogeneous dispersion studies using physical mixing and sonication, stock solutions were prepared either in PBS or deionized water. The stock solutions of Fe_3O_4 (30, 47 nm), TiO_2 (40 nm) and CdO (1000 nm) particles were homogeneously dispersed in PBS while Ag (15, 100 nm) particles were suspended in deionized water. From this stock solution different final concentrations were prepared in cell growth medium (Ham's Nutrient Mixture F-12) without serum. It was noted that turbidity increased with increasing concentration of nanomaterials. The turbidity intensified significantly at the 250 μg/ml in all of the nanoparticles solutions. Another physical observation was that Ag-100 rapidly settled out of dispersed solution suspension and constant mixing was necessary before adding it to the exposure media. Ag-100 nm was not homogenously suspended in solution as evidenced by nanoparticles settling to the bottom of the bottle.

2.3. Cell culture

BRL 3A (ATCC, CRL-1442) immortalized rat liver cells were used between passages 10 and 20. BRL 3A cells were grown in culture media with 5% fetal bovine serum. Cells were plated at a density in 6 or 24-well plates for confluency exposures by 36–48 h when dosing with nanoparticles was initiated. The cells were maintained in a 5% CO_2 incubator at 37 °C.

2.4. Treatment protocol

After the monolayer of cells became confluent in 6 or 24-well plate, BRL 3A cells were treated with a range of concentrations of nanoparticles suspended in Ham's Nutrient Mixture F-12 without serum for 24 h. After the 24 h treatment, the various toxicity end points were evaluated in control and nanoparticle-exposed cells.

2.5. Qualitative observation of external morphology by phase contrast inverted microscopy

BRL 3A cells were exposed as mentioned above at various concentrations of nanoparticles for 24 h. After completion of the exposure period, cells (control and exposed) were washed with PBS and observed by phase contrast inverted microscopy at 100× magnification.

2.6. Cytotoxicity endpoints

LDH leakage due to membrane damage was assessed by measuring the activity of LDH in the cells and media as described elsewhere with some modifications

(Hussain and Frazier, 2002). Mitochondrial function was evaluated spectrophotometrically by measuring the degree of mitochondrial reduction of the tetrazolium salt 3-(4,5-dimethylthiazol-2-yl)-2,5-diphenyltetrazolium bromide (MTT) to (aqueous insoluble product) formazan by succinic dehydrogenase (Carmichael et al., 1987) with minor modification as described elsewhere by Hussain and Frazier, 2002. ROS generation was determined using dichlorodihydrofluorescein diacetate (H_2 DCFDA) (Wang and Joseph, 1999) with minor modifications as previously described by Hussain and Frazier, 2002. Mitochondrial membrane potential was determined by the uptake of rhodamine 123 (Molecular Probes, Inc., Eugene, OR) according to the method of Wu et al. (1990). Reduced glutathione (GSH) was measured in 96-well plates using a SpectraMAX Plus 190 microplate reader (Molecular Devices, Sunnyvale, CA) according to the procedures described in the Glutathione Assay Kit (Cayman Chemical Company, Ann Arbor, MI).

2.7. Statistical evaluation

The data were expressed as mean ± standard deviation (SD) of three independent experiments. Wherever appropriate, the data were subjected to statistical analysis by one-way analysis of variance (ANOVA) followed by Dunnett's method for multiple comparisons. A value of $p < 0.05$ was considered significant. SigmaStat for Windows version 2.03 software was used for the statistical analysis.

3. Results

The results demonstrated that exposure to Ag nanoparticles for 24 h resulted in concentration-dependent increase in LDH leakage and exhibited a significant ($p < 0.05$) cytotoxicity at 10–50 μg/ml (Fig. 1B). It was noted that there is a statistically significant difference between different silver particle sizes of 100 and 15 nm,

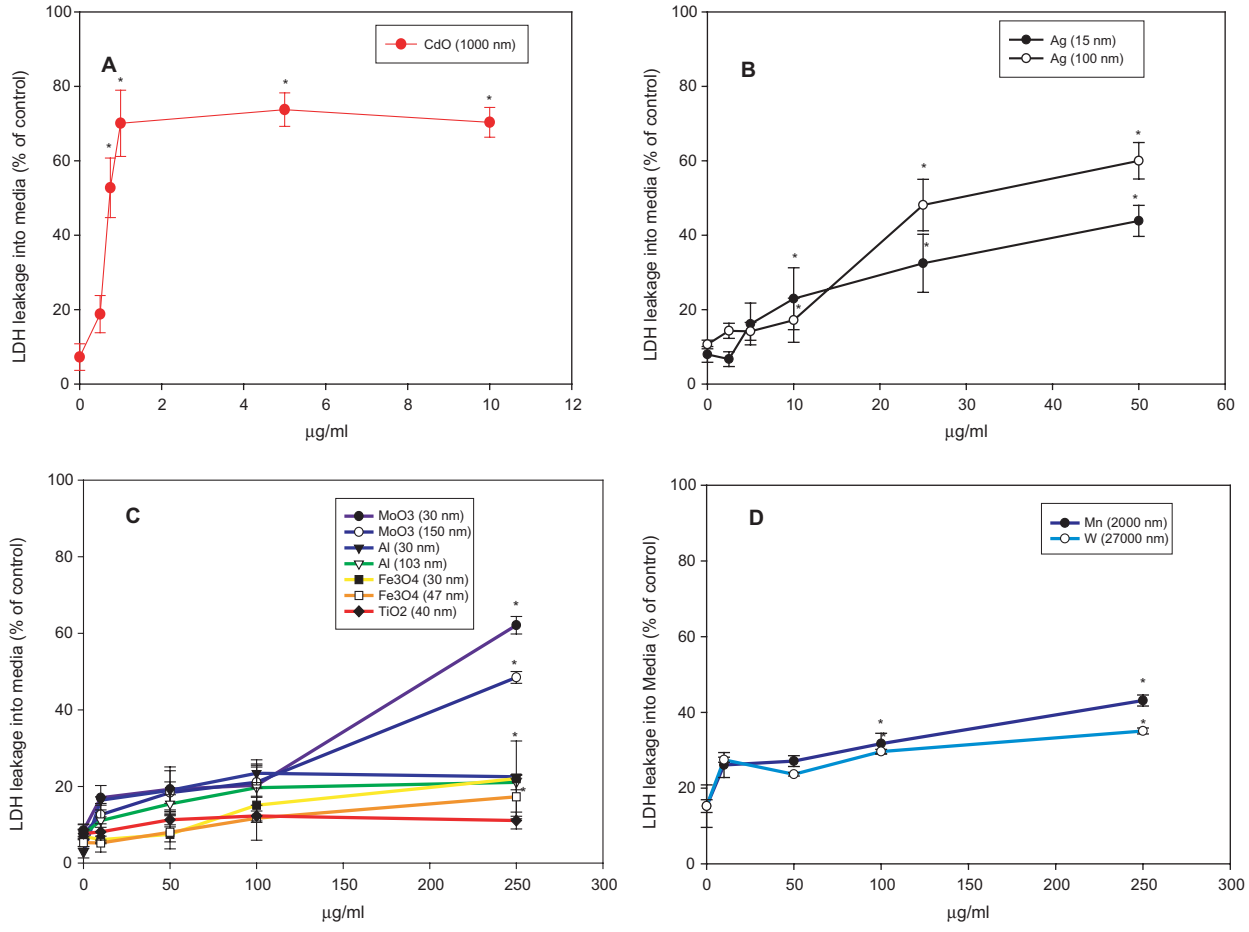

Fig. 1. Effect of nanoparticles on LDH leakage in rat liver cells BRL 3A cells. Cells were treated with different concentrations of nanoparticles for 24 h. At the end of the incubation period, the LDH assay was performed to assess the LDH leakage as described in Section 2. The percent of LDH activity was then calculated by dividing the amount of activity in the medium by the total activity (medium and cell lysate). Control cells were cultured in nanoparticle-free media were run in parallel to treatment groups. The data are expressed as mean ± SD of three independent experiments. (*) indicates a statistically significant difference compared to controls ($p < 0.05$).

where the 100 nm particles showed higher toxicity at 25 and 50 μg/ml. The results for LDH leakage for MoO_3, Al, Fe_3O_4, MnO_2, W, nanoparticles exposure did not produce cytotoxicity up to the concentration of 100 μg/ml (Fig. 1C and D), but it produced a significant effect at 250 μg/ml. There was no significant difference when comparing the toxic effects between different sizes of Fe_3O_4 nanoparticles (30 nm versus 47 nm) (Fig. 1C). Based on LDH results, the most toxic nanomaterial was Ag (15, 100 nm) when compared to other nanomaterials. The CdO was used only as a positive control for significant toxicity at low doses (0.5 μg/ml) (Fig. 1A).

The results of MTT assays showed Ag exposure exhibited a significant cytotoxicity from 5 to 50 μg/ml (Fig. 2B; Table 1). In contrast, the other nanoparticles did not produce a significant increase in cytotoxicity at the doses tested (Fig. 2C and D) except at 250 μg/ml. The larger microparticles (W-27000 nm) showed toxicity at 100 μg/ml while (MnO_2-2000 nm) was toxic at 250 μg/ml. There was a slight increase in mitochondrial function at the 10 μg/ml doses of MoO_3 and Fe_3O_4 nanoparticles, but these were not statistically significant (Fig. 2C). There was relatively no change in MTT measurement indicating that the mitochondrial function was not altered at these doses. The MTT assay showed silver nanoparticles are more toxic than other nanoparticles. The EC_{50} values of MTT

Table 1
Calculated EC_{50} values of Nanoparticles: EC_{50} values represent effective concentration of nanoparticles that increases LDH leakage to 50% or decreases MTT reduction by 50%

Chemical	MTT EC_{50}, μg/ml	LDH EC_{50}, μg/ml
CdO (1000 nm)	0.83 ± 0.027	0.75 ± 0.052
Ag (100 nm)	19 ± 5.2	24 ± 9.25
Ag (15 nm)	24 ± 7.25	50 ± 10.25
MoO_3 (150 nm)	174.68 ± 26	250 ± 17
MoO_3 (30 nm)	171.58 ± 25	210 ± 30
Fe_3O_4 (30, 47 nm); Al (103 nm); MnO_2 (2000 nm); W (27000 nm)	>250	>250

Values were calculated by using linear statistical regression analysis.

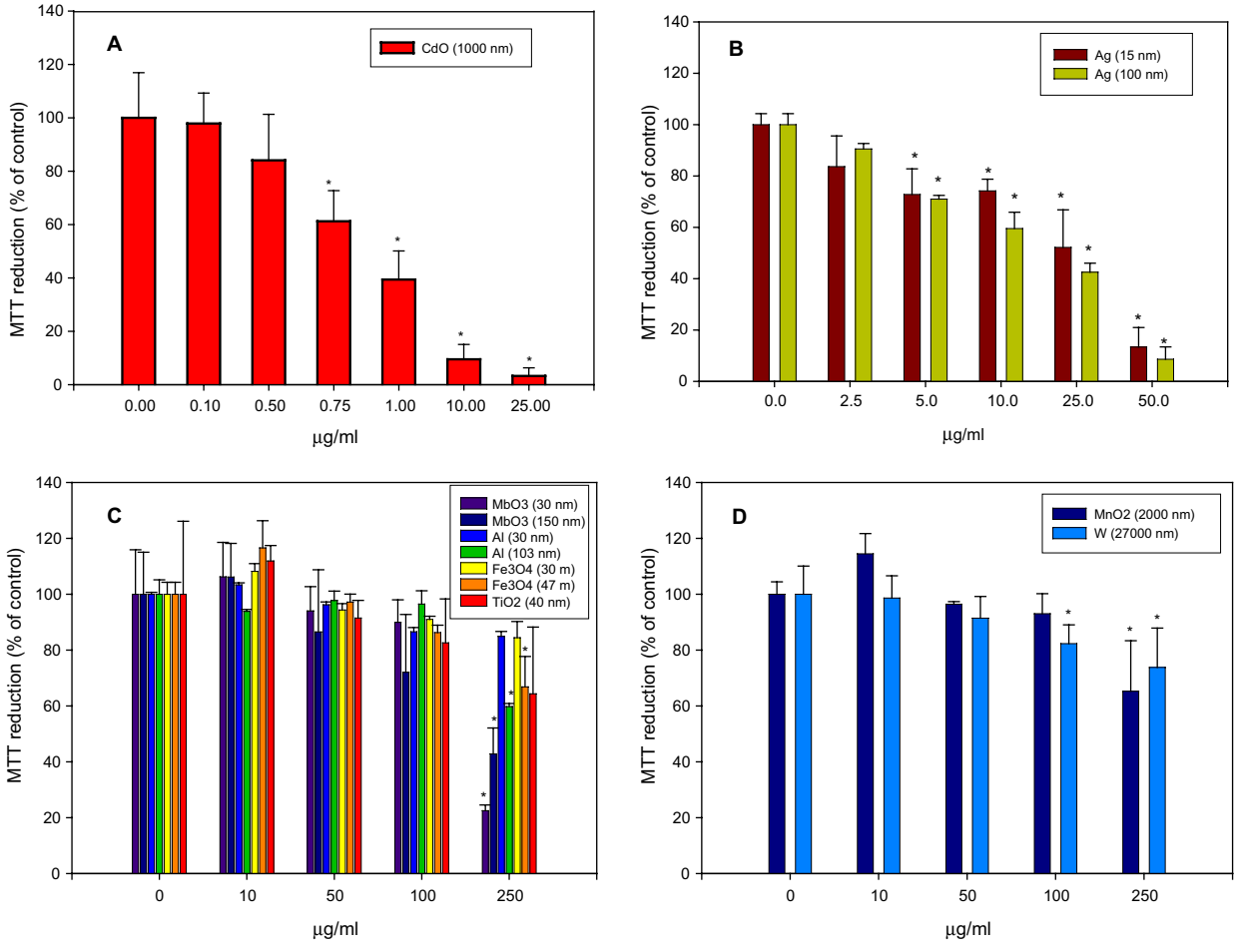

Fig. 2. Effect of nanoparticles on mitochondrial function in rat liver cells (BRL 3A cells). Cells were treated with different concentrations of nanoparticles for 24 h. At the end of the incubation period, mitochondrial function was determined by the MTT reduction assay as described in Section 2. The subtracted OD value of control cells (nanoparticle-free medium at 0 h) was taken as 100% and then calculated as the percentage of reduction of OD in nanoparticle-exposed cells. Control cells cultured in nanoparticles-free media were run in parallel to treatment groups. The data are expressed as mean ± SD of three independent experiments. (*) indicates a statistically significant difference compared to controls ($p < 0.05$).

calculated to be 24 and 19 μg/ml for Ag-15 and Ag-100 nanoparticle respectively (Table 1). However, EC_{50} values were higher for other nanoparticles.

Based on the above results it is apparent that Ag was the most toxic material, therefore, further study with silver toxicity was conducted to elucidate a general mechanism of toxicity with reference to oxidative stress. To investigate the potential role of oxidative stress as a mechanism of toxicity of Ag (15, 100 nm), the effects produced on ROS, MMP and GSH were studied.

Fig. 3A shows the general external morphology of control cells and Ag nanoparticle-exposed cells. The Ag (15, 100 nm) nanoparticles appeared to be associated with cells exhibiting a blackish or reddish color when observed under the microscope. At the low dose (10 μg/ml), the cells appear similar to control cells with brownish particles most likely associated with the cell membranes. With increasing doses of Ag nanoparticles, the BRL 3A cells started to shrink and became irregular in shape (Fig. 3C and E). These microscopic studies

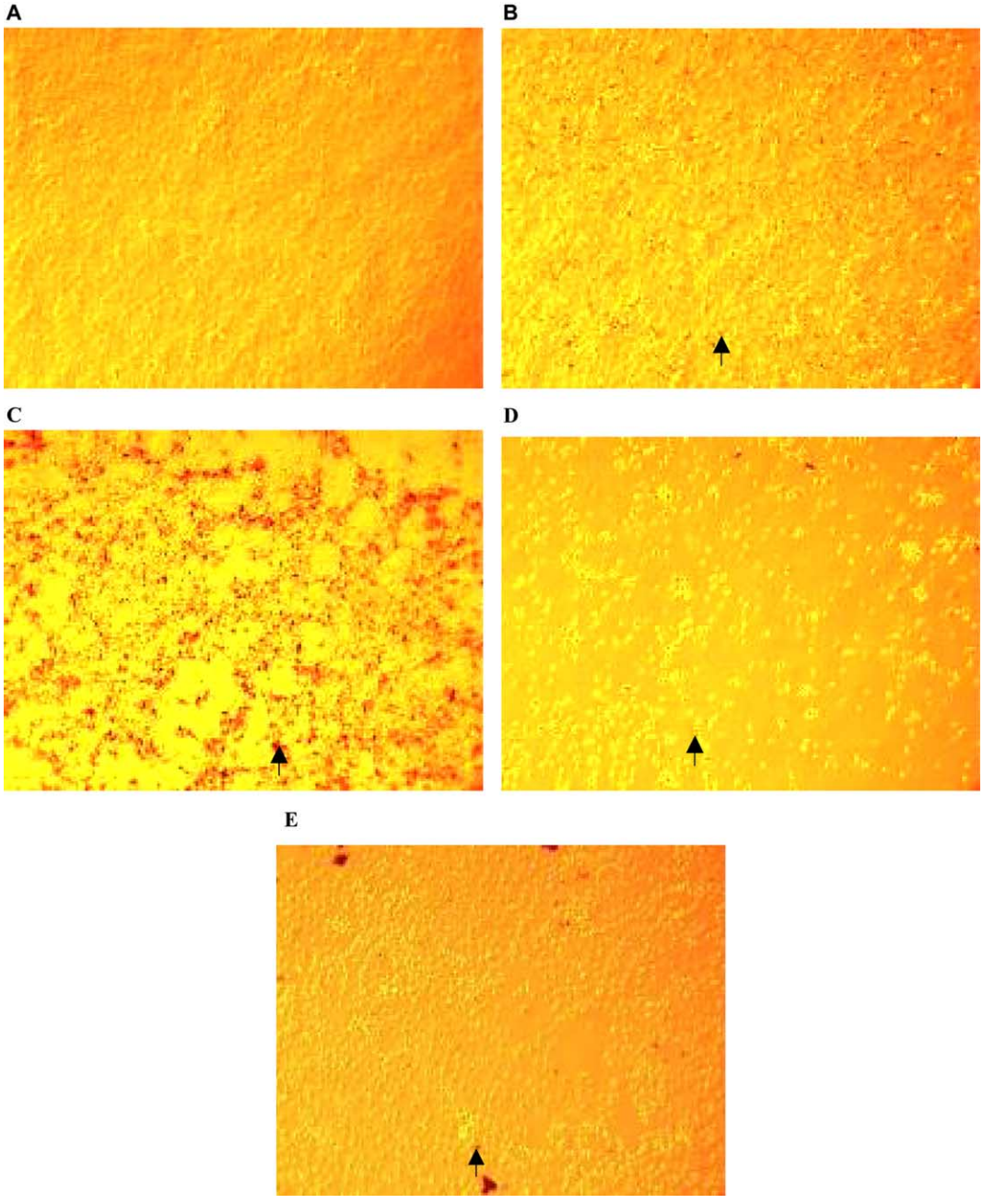

Fig. 3. Morphological characterization of rat liver cells (BRL 3A cells). Cells were treated with different concentrations of Ag (15 and 100 nm) in Ham's Media and incubated for 24 h at 37 °C in a 5% CO_2 atmosphere. At the end of 24 h exposure cells were washed with PBS and the cells were visualized by inverted microscope (magnification 10×). (A) Control; (B) 25 μg/ml of Ag 15 nm; (C) 50 μg/ml of Ag 15 nm; (D) 25 μg/ml of Ag 100 nm and (E) 50 μg/ml of Ag 100 nm. Arrow indicates silver particle associated with cells.

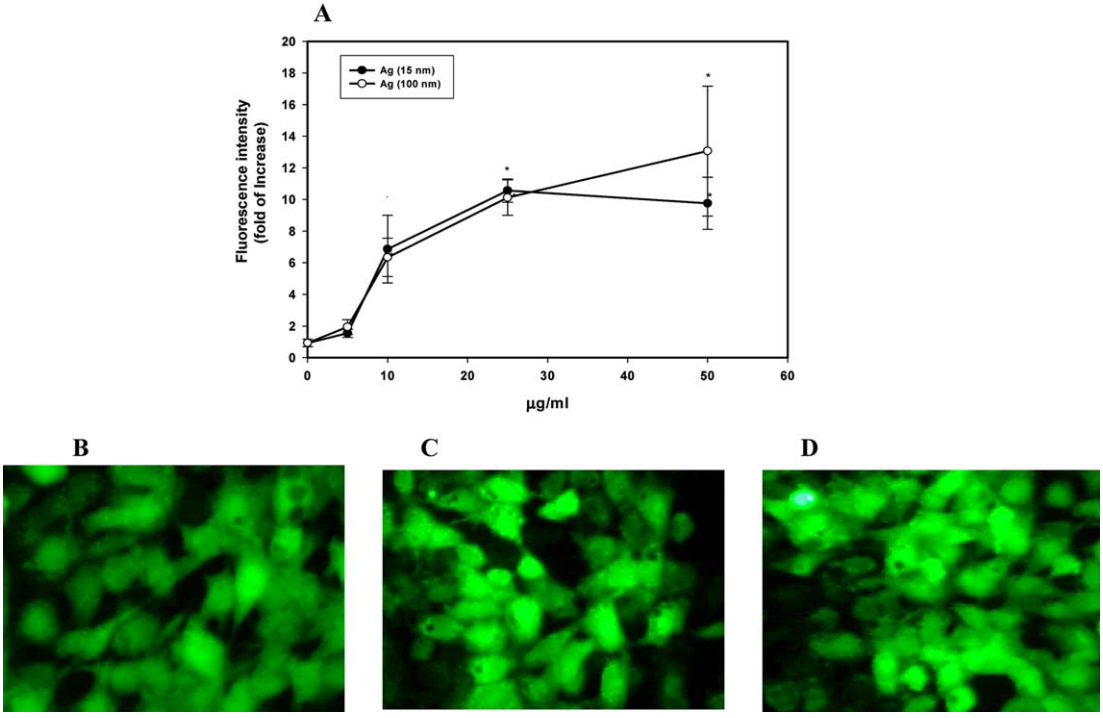

Fig. 4. (A) Effect of Ag (15, 100 nm) on ROS generation in rat liver cells (BRL 3A cells). Cells were incubated with 20 μM of DCFH-DA for 30 min in a 96-well plate. After DCFH-DA containing medium was removed, the cells were washed with PBS and treated with Ag (15, 100 nm) in exposure media for 6 h. At the end of exposure, dichloro-fluorescein fluorescence was determined at excitation wavelength 485 nm and emission wavelength 530 nm. Data are reported as fold increase in fluorescence intensity relative to control. Control cells cultured in Ag (50, 100 nm)-free media were run in parallel to treatment groups. The data are expressed as mean ± SD of three independent experiments. (∗) indicates a statistically significant difference compared to controls ($p < 0.05$). (B–D) Qualitative characterization of ROS generation by DCFH-DA staining using fluorescence microscopy. Cells were incubated with 20 μm of DCEF as described in (A). At the end of 6 h exposure cells were washed with PBS and the cells were visualized by fluorescence microscopy (Nikon, Eclipse TS 100 (×200)) at excitation wavelength of 485 nm and an emission wavelength of 530 nm. (B) Control; (C) 25 μg/ml Ag-15 nm; (D) 25 μg/ml Ag-100 nm.

indicate that not all nanoparticles accumulated in the cells, rather some associated with membranes.

ROS generation following 6 h of exposure to Ag (15, 100 nm) at 0, 5, 10, 25, and 50 μg/ml is shown in Fig. 4A–D. The maximum ROS levels were found at 6 h, from that point on the levels of ROS reduced over a period of 24 h (data not shown). Therefore, the data shown here was only at 6 h exposure. The level of ROS in cells increased in a concentration-dependent manner and was statistically increased ($p < 0.05$) from 10 μg/ml concentration. Ag (15, 100 nm) treatment at 25 and 50 μg/ml resulted in an approximately 10-fold increase in ROS generation over control levels (Fig. 4A). The qualitative generation of ROS was also observed using fluorescence microscopy, which detected the brightest obvious fluorescent intensity with Ag exposed cells at 25 μg/ml (Fig. 4B–D).

The effect of Ag (15, 100 nm) on mitochondrial membrane potential (MMP) was evaluated in BRL 3A cells (Fig. 5A–D). Cells were exposed to 0, 5, 10, 25, and 150 μg/ml Ag (15, 100 nm) for 24 h and immediately assayed for rhodamine 123 uptake. The results indicated that there was a significant decrease (80%) of MMP at 25 and 50 μg/ml Ag (15, 100 nm) (Fig. 5A). The qualitative mitochondrial membrane potential was also observed under fluorescence microscope stained with rhodamine 123. The brightness of the fluorescent intensity was reduced in cells exposed to Ag at 25 and 50 μg/ml that indicates a significant reduction of mitochondrial membrane potential (Fig. 5B–D).

Glutathione (GSH) is a ubiquitous sulfhydryl-containing molecule in cells that is responsible for maintaining cellular oxidation–reduction homeostasis (Sies, 1999). Alterations in GSH homeostasis can be monitored as an indication of functional-damage to cells. A significant depletion of GSH (70%) was observed at 25 μg/ml Ag (15,100 nm) relative to controls (61.00 ± 5.28 nmol GSH/mg cellular protein) (Fig. 6). Overall, the data demonstrated a significant depletion ($p < 0.05$) of GSH levels occurred in Ag (15,100 nm) exposed cells.

4. Discussion

The purpose of this investigation was to evaluate potential toxicity and the general mechanism involved in nanoparticle toxicity. To date there are very few studies directly or indirectly investigating the toxic effects of

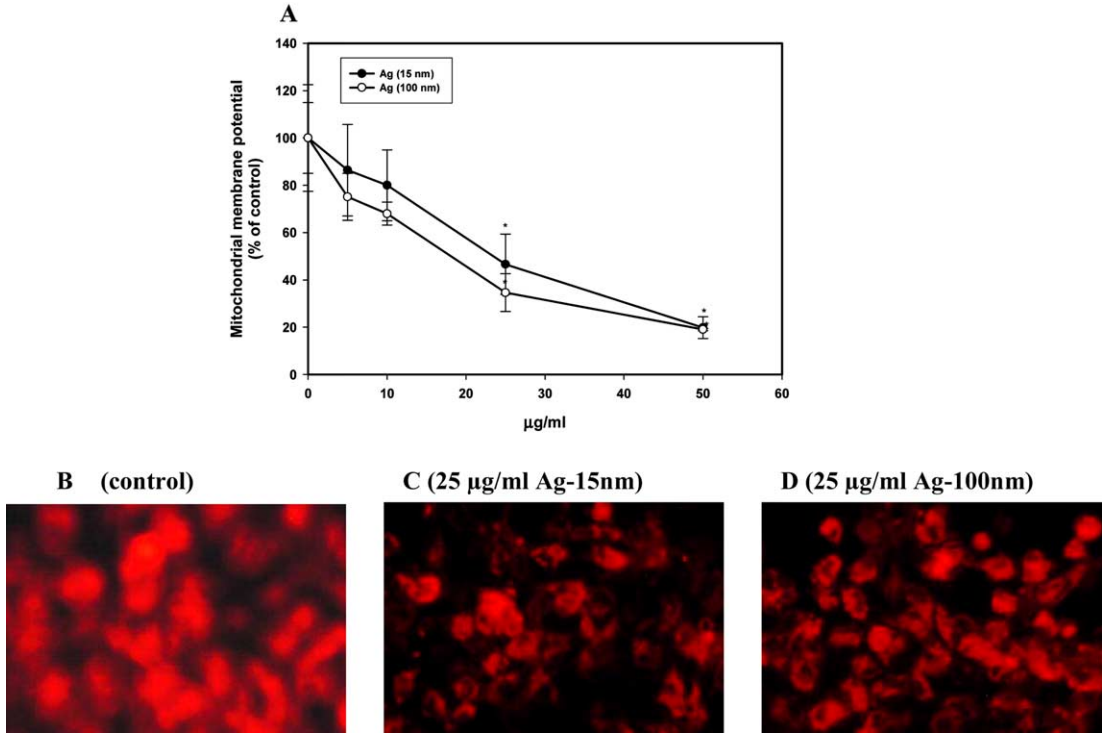

Fig. 5. (A) Effect of Ag (15, 100 nm) on mitochondrial membrane potential in rat liver cells (BRL 3A cells). Cells were exposed to different concentrations of Ag (15, 100 nm) for 24 h. After 24 h exposure cells were incubated with rhodamine 123 for 30 min in a 96-well plate then cells were washed with PBS. The fluorescence was determined at excitation wavelength 485 nm and emission wavelength 530 nm. Control cells cultured in Ag (50, 100 nm)-free media were run in parallel to treatment groups. The fluorescence intensity value of control cells (nanoparticle-free medium at 0 h) was taken as 100% and then calculated as the percentage of reduction of fluorescence in nanoparticle-exposed cells. Data are expressed as percent of control as mean ± SD of three independent experiments. (∗) indicates a statistically significant difference compared to time-matched controls ($p < 0.05$). (B–D) Qualitative characterization of mitochondrial membrane potential by rhodamine 123 staining using fluorescence microscopy. Cells were incubated with rhodamine 123 as described in Fig. 4A. At the end of rhodamine 123 cells were washed with PBS and the cells were visualized by fluorescence microscopy (Nikon, Eclipse TS 100 (×200)) at excitation wavelength of 485 nm and an emission wavelength of 530 nm.

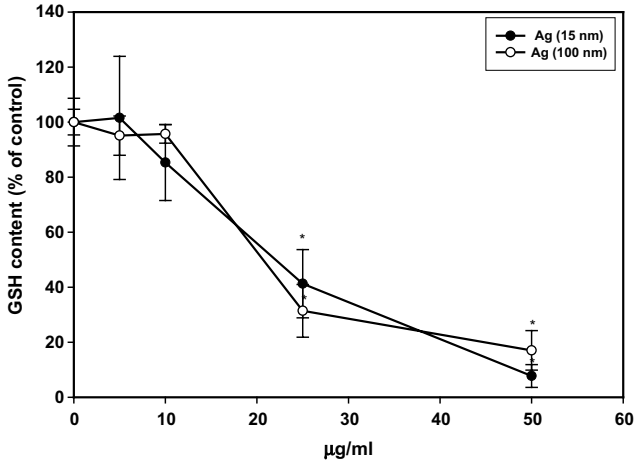

Fig. 6. Effect of Ag (15, 100 nm) on GSH levels in rat liver cells (BRL 3A cells). Cells were treated with different concentrations of Ag (15, 100 nm) for 24 h. At the end of the exposure, cells were washed with PBS, and GSH (control: 61.00 ± 5.28 nmol/mg protein) levels were measured as described in Section 2. Control cells cultured in Ag (50, 100 nm)-free media were run in parallel to treatment groups. The data are expressed as mean ± SD of three independent experiments. (∗) indicates a statistically significant difference compared to controls ($p < 0.05$).

nanomaterials and no clear guidelines are presently available to quantify these effects. Recently, Lam et al. (2004) reported that nanotubes induced lung tissue damage in mice resulting in granulomas. Another report by Warheit et al. (2004) investigated acute lung toxicity and observed that intratracheally instilled single-wall carbon nanotubes produced granulomas in rats at very high doses. The current study aimed to investigate the toxicity of nanoparticles in an in vitro model derived from rat liver cells BRL 3A. These cell lines have been well characterized for their relevance for toxicity studies (Boess et al., 2003).

We have recently reported the results of cytotoxicity testing of series of high energy chemicals in an in vitro model (Hussain and Frazier, 2001, 2002), and these data were used to derive a baseline for extrapolation to a human health risk assessment (Trohalaki et al., 2002). Although, in vitro data is not a substitute for whole animal studies, use of simple in vitro models with end points that reveal a general mechanism of toxicity can be a basis for further assessing the potential risk of chemical/material exposure. As far as the assessment of toxicological properties of nanoparticles is concerned, it is not

known how they behave when they are dispersed in exposure media. Some of the nanomaterials settled rapidly and needed constant stirring to make a homogeneous suspension, and the full cellular dose/time of these materials would be larger. The other issue that is still not known is whether the cells internalize nanoparticles, and if so, what are the mechanisms involved. Our results of microscopic studies showed that nanoparticles associate with cell membranes and that the cells internalize some of the particles. This is very evident in alveolar macrophages where nanoparticles are surrounded within cells (manuscript in preparation). The nanoparticles associated with cell membrane or entering into cells are likely to have an effect on cellular function.

The results observed for the biochemical endpoints described in this paper demonstrate that Ag (15, 30 nm) nanomaterials increase LDH leakage and reduces MTT reduction in a dose dependent manner over a 24 h exposure duration. However, the other nanomaterials showed toxicity at higher doses of 100 μg/ml or above. Micrometer-sized CdO, which is not purported to be a production material, was considered as a positive control, and its exposure demonstrated a dose response toxicity at very low exposure doses. It is unknown if this compound has a significant dissolution rate within cultured cells, or gains access into internal cellular matrix. Further investigation of smaller sized CdO is merited to determine effect of size and distribution of this toxic material. The TiO_2 was used as negative control based on published ultrafine irritancy particle results that shows no toxicity to these cells (Lee et al., 1985). Overall, the data based on MTT and LDH assays suggest that Ag was highly toxic whereas MoO_3 was moderately toxic and Fe_3O_4, Al, MnO_2 and W displayed less or no toxicity at the doses tested.

Further studies were conducted with silver particles to elucidate a general mechanism with reference to oxidative stress. The recent study by Oberdörster (2004) indicated that nanomaterials (Fullerences C_{60}) induced oxidative stress in a fish model, as demonstrated by a significant elevation of lipid peroxidation and marginal GSH depletion. Our results here show that there was a significant increase in ROS at 10, 25 and 50 μg/ml of Ag (15, 100 nm). ROS generation increased with exposure concentration up to 25 μg/ml, with no further increase at 50 μg/ml. This lack of increase in ROS at the higher exposure concentrations may be a consequence of the leakage of fluorescent product from the cell, since evidence of significant membrane damage (LDH leakage) was apparent at the highest concentration. Increased generation of ROS by Ag (15, 100 nm) is likely to contribute to oxidative stress that may ultimately lead to the observed cytotoxicity. It is noted that the 25 and 50 μg/ml concentration of Ag (15, 100 nm) depleted GSH significantly. Several questions arise as to how nanoparticles could induce toxicity. It is not known, for instance, how Ag (15, 100 nm) depletes GSH levels, whether it binds directly to GSH, or inhibits enzymes involved in GSH synthesis. GSH depletion in liver cells exposed to Ag (15, 100 nm) is strongly correlated with increased ROS generation. It is possible that the loss of GSH may compromise cellular antioxidant defenses and lead to the accumulation of reactive oxygen species (ROS) that are generated as by-products of normal cellular function. Whether any signaling pathways are involve in nanomaterials-induced toxicity is not known. Since these are relatively new particles, it is necessary to investigate their toxicological behavior and this first report provides such preliminary information in this direction.

In summary nanoparticles lead to cellular morphological modifications, LDH leakage and mitochondrial dysfunction, and Ag (15, 100 nm) in particular, cause increased generation of ROS, depletion of GSH, and reduction of mitochondrial membrane potential. Our preliminary data suggest that oxidative stress is likely to contribute to nanoparticle cytotoxicity. Further studies are underway to investigate the mechanism to see if apoptosis is involved in nanoparticle toxicity.

Acknowledgements

This work was supported by the Air Force Office of Scientific Research (AFOSR) Project (JON# 2312A211) and performed in conjunction with U.S. Air Force Contract F41624-96-C-9010 (ManTech/Geo-Centers Joint Venture). We are thankful to our Division Chief Col Riddle for his strong support and encouragement. The authors are thankful to Dr. Marie Claude-Hofmann, University of Dayton for helping fluorescence microscopic work.

References

Boess, F., Kamber, M., Romer, S., Gasser, R., Muller, D., Albertini, S., Suter, L., 2003. Gene expression in two hepatic cell lines, cultured primary hepatocytes, and liver slices compared to the in vivo liver gene expression in rats: possible implications for toxicogenomics use of in vitro systems. Toxicological Sciences 73, 386–402.

Bruchez, M., Moronne, M., Gin, P., Weiss, S., Alivisatos, A.P., 1998. Semiconductor nanocrystals as fluorescent biological labels. Science 281, 2013–2016.

Carmichael, J., DeGraff, W.G., Gazdar, A.F., Minna, J.D., Mitchell, J.B., 1987. Evaluation of a tetrazolium-based semiautomated colorimetric assay: assessment of chemosensitivity testing. Cancer Research 47, 936–942.

Colvin, V., 2003. The potential environmental impacts of engineered nanomaterials. Nature Biotechnology 21, 1166–1170.

Cui, Y., Wei, Q., Park, H., Lieber, C., 2001. Nanowire nanosensors for highly sensitive and selective detection of biological and chemical species. Science 293, 1289–1292.

Foley, S., Crowley, C., Smaihi, M., Bonfils, C., Erlanger, B., Seta, P., et al., 2002. Cellular localisation of a water-soluble fullerene derivative. Biochemical and Biophysical Research Communications 294, 116–119.

Hussain, S.M., Frazier, J.M., 2001. In vitro assessment of high energy chemicals in rat hepatocytes. The Science of the Total Environment 274, 151–160.

Hussain, S.M., Frazier, J.M., 2002. Cellular toxicity of hydrazine in primary hepatocytes. Toxicological Sciences 69, 424–432.

Jani, P., Halbert, GW., Langridge, J., Florence, AT., 1990. Nanoparticle uptake by the rat gastrointestinal mucosa: quantitation and particle size dependency. Journal of Pharmacy Pharmacology 42, 821–826.

Oberdörster, E., 2004. Manufactured nanomaterials (Fullerenes, C_{60}) induce oxidative stress in the brain of juvenile largemouth bass. Environmental Health Perspectives 112, 1058–1062.

Lam, C.-W., James, J.T., McCluskey, R., Hunter, R.L., 2004. Pulmonary toxicity of single-wall carbon nanotubes in mice 7 and 90 days after intratracheal instillation. Toxicological Sciences 77, 126–134.

Lee, K.P., Trochimowicz, H.J., Reinhardt, C.F., 1985. Pulmonary response of rats exposed to titanium dioxide (TiO2) by inhalation for two years. Toxicology and Applied Pharmacology 79, 179–192.

Sies, H., 1999. Glutathione and its role in cellular functions. Free Radical Biology and Medicine 27, 916–921.

Taton, T., Mirkin, C., Letsinger, R., 2000. Scanometric DNA array detection with nanoparticle probes. Science 289, 1757–1760.

Trohalaki, S., Pachter, R., Hussain, S., Frazier, J., 2002. Quantitative structure activity relationships (QSARS) for high-energy chemicals. Toxicological Sciences 68, 498–507.

Wang, H., Joseph, J.A., 1999. Quantitating cellular oxidative stress by dicholorofluorescein assay using microplate reader. Free Radical Biology and Medicine 27, 612–616.

Warheit, D.B., Laurence, B.R., Reed, K.L., Roach, D.H., Reynolds, G.A.M., Webb, T.R., 2004. Comparative pulmonary toxicity assessment of single-wall carbon nanotubes in rats. Toxicological Sciences 77, 117–125.

Wu, E.Y., Smith, M.T., Bellomo, G., Di Monte, D., 1990. Relationships and cytotoxicity in isolated rat hepatocytes. Archives of Biochemistry and Biophysics 282, 358–362.